

## FLOW EFFECTS AND MODELING IN GAS-COOLED QUENCHING

Mats Lind

Faxén Laboratory  
Royal Institute of Technology  
S-100 44 Stockholm  
Sweden

Farid Alavyoon

Vattenfall Utveckling AB  
S-810 70 Älvkarleby  
Sweden

Noam Lior

Dept. of Mechanical Engng and Appl. Mech.  
University of Pennsylvania  
Philadelphia, PA 19104-6315  
U.S.A.

Fritz Bark

Faxén Laboratory  
Royal Institute of Technology  
S-100 44 Stockholm  
Sweden

### INTRODUCTION

Environmental problems associated with the use of oils and other liquids in the quenching of steel have been one of the primary motivators for the increased interest in their replacement by inert gases, such as nitrogen, helium and hydrogen (cf. Midea et al., 1996). When oil or other liquids are used for quenching, the primary heat transfer mode between the quenched metal and the liquid is boiling, which produces very high heat transfer coefficients. The convective heat transfer coefficients between gas and solid are, however, at least one to two orders of magnitude lower. Consequently, to obtain higher heat transfer coefficients in gas-quenching it is necessary to use high gas velocities, which unfortunately result in severe variations of these coefficients along the quenched surface, and in rather large energy consumption by the gas blowers. The former problem causes nonuniformities in the temperature distribution in the quenched body, with consequently undesirable distortions, residual stresses, and nonuniformities in its mechanical properties (cf. Inoue & Wang, 1985, Sjöström, 1985, Fletcher, 1989, Thuvander & Melander, 1993).

To illustrate the problem, Fig. 1 demonstrates the flow, heat transfer and nonuniformities as computed by us for the convective-conductive problem (details are in the Section on numerical flow modeling) for cross-flow quenching of a stainless steel cylinder initially at 1200 K, by means of nitrogen at 10 bar 300 K, with  $Re = (3.16)10^5$ ,  $Pr = 0.7$ ,  $Bi = 0.66$ , at  $Fo = 0.27$ . The boundary layer thickens from the stagnation point downstream, until separation is seen to occur at about  $100^\circ$ , followed by a recirculation zone and wake.  $h$  is seen to be, as expected, high in the stagnation region, gradually decreasing downstream as the boundary layer thickens, rising to a maximum in the flow separation region, then decreasing, and further downstream slightly increasing in the wake region.

The primary objective of this study is to examine the effects of the nature of the cooling-gas flow on the transient internal temperature distribution in metals during quenching. To that end we first examine generically the effects of nonuniformity of convective heat transfer coefficients on the internal temperature

distribution, and then we examine the suitability of several  $k-\epsilon$  turbulent flow models for the computation of these coefficients.

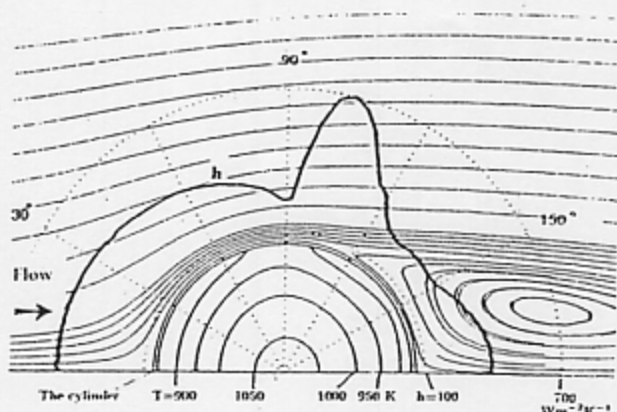


Figure 1: Typical velocity ( $U^*$ ), surface convective heat transfer coefficient ( $h$ ), and internal temperature ( $T$ ) distributions as computed for the cross-flow quenching of a stainless steel cylinder.  $T_{ci} = 1200$  K,  $T_f = 300$  K,  $k_s = 20$  W m<sup>-1</sup>K<sup>-1</sup>,  $Re = (3.16)10^5$ ,  $Pr = 0.7$ ,  $Bi = 0.66$ ,  $Fo = 0.27$ .

### SENSITIVITY OF THE INTERNAL TEMPERATURE DISTRIBUTION TO THE SURFACE CONVECTIVE HEAT TRANSFER COEFFICIENT DISTRIBUTION

The temperature distribution uniformity and the magnitude of the temperature gradients in the quenched solid have a primary effect on distortions and residual stresses. On the path to determining the effect of the cooling gas flow on these undesirable phenomena, it is thus easier and rather useful to first find the sensitivity of these temperature distributions and gradients to the surface heat transfer coefficient distribution. The temperature distributions in two practical body shapes, a long cylinder and a long rod with a square cross-section, subjected to several convective heat transfer coefficient distributions as

detailed below, have thus been computed, and the results are shown in Figs. 2 and 3.

In addition, the volume-average of the absolute values of the temperature gradients  $|\nabla T|$ , the magnitude and location of the maximal temperature gradients  $(\nabla T)_{\max}$ , and a heat-treatment

figure of merit  $\Gamma \equiv \frac{\dot{q}_c \left(\frac{A}{V}\right)^2}{k_s |\nabla T|}$  that we have defined, have been

calculated. In heat treatment it is typically desirable to have high overall cooling rates yet low temperature gradients, thus higher values of  $\Gamma$  imply a better heat treatment process. Similarly, a higher surface-to-volume ratio is more desirable in quenching, and it was raised in this definition to the second power so that  $\Gamma$  would become dimensionless. We note that while temperature gradients have a primary role in generating distortions, residual stresses and problems with the final mechanical properties of the quenched object, due to thermal stresses and peculiarities in the crystalline phase transformations, these undesirable effects are affected by other parameters too. Our analysis thus provides a preliminary good insight into the problem, but a full analysis of the conjugate flow, heat transfer, elasto-plastic behavior, and phase change problem must be conducted for more precise results, and it is indeed under way at the Faxén Laboratory and elsewhere (cf. Thuvander & Melander 1993, Inoue et al., 1996, Dowling et al., 1996).

Figure 2 shows the conditions and results during quenching of a long cylinder. The  $h$  distributions used are: in the first column (a) uniform  $h$  along the surface, at a value comparable to that obtained for practical gas quenching; in the second column (b) values of  $h$  computed by us using the LSY-CG version of the  $k$ - $\epsilon$  turbulent flow model for  $Re = (3.16)10^3$ ,  $Pr = 0.7$ , with details discussed in the following section; and in the third column (c), the experimental values of Žukauskas and Žiugžda (1984) for the same conditions.

As expected, a uniform  $h$  produces a uniform temperature distribution in this fully symmetric body cross section. Regions of lower  $h$  (such as in  $60^\circ$ - $90^\circ$  in Fig. 2b and  $70^\circ$ - $90^\circ$  in Fig. 2c) produce regions of smaller internal temperature gradients, while regions of higher  $h$  ( $95^\circ$ - $105^\circ$  in Fig. 2b and  $\sim 115^\circ$  in Fig. 2c) produce regions of higher internal temperature gradients. Notably, internal temperature gradient asymmetries are generated by the nonuniformities in  $h$ . In addition to the magnitude of the temperature gradient, such asymmetries, if of sufficient strength, would give rise to distortion.

The quenching figure of merit  $\Gamma$  shows small but physically-consistent changes between the different  $h$  distributions:  $\Gamma$  increases with increased uniformity of  $h$ , and it decreases with time. The maximal gradient,  $(\nabla T)_{\max}$ , is located on the cylinder surface at  $\phi = 120^\circ$  for the experimentally-obtained values of  $h$  (Fig. 2c), and at  $\phi = 107^\circ$  when the  $h$  is predicted by simulation (Fig. 2b). It increases significantly with the nonuniformity of  $h$ , by up to 56% in the considered range of parameters, as compared with the uniform  $h$  distribution. Even the relatively small increase in nonuniformity due to numerical model inadequacy (comparing Figs 2b and 2c) is seen to cause an increase of up to 28% in  $(\nabla T)_{\max}$ .

Preliminary numerical analysis of cross flow of gas over hotter prismatic objects (such as the rod of rectangular cross section in Fig. 3) have indicated that  $h$  in many cases tends to be lower near

the corners (where separation typically occurs) than at the center of each face (stagnation). We have thus applied three somewhat arbitrary distributions of  $h$  to a steel bar of rectangular cross section; a linear one (Fig. 3b) and a quadratic (Fig. 3c) which follow this pattern, and a uniform  $h$  (Fig. 3a) for comparison. For simplicity, the heat conduction analysis was performed on only 1/8 of the cross section, with each vertical line in Fig. 3 being half the centerline of the corresponding square. The average magnitude of  $h$  in all cases is a practical  $300 \text{ W m}^{-2} \text{ K}$ .

In general,  $\Gamma$  behaves in a way similar to that exhibited with the cylinder. It is the highest for the uniform  $h$  (Fig. 3a), lower for the linear distribution of  $h$  (Fig. 3b) and lowest for the quadratic distribution of  $h$  (Fig. 3c).  $(\nabla T)_{\max}$  is also located on the surface, always at the center of the face, is also lowest for the uniform distribution of  $h$ , but is highest, by 2.5-fold, for the quadratic distribution of  $h$ .

Probably the most notable observations from the analysis are (1) as expected and in contrast with the cylindrical cross section, the isotherms here are not parallel to the body contour, creating different temperatures and gradients along the surface even for a uniform  $h$ , and (2) while a uniform  $h$  makes the corners coldest, application of the more realistic distributions of  $h$  reverses this behavior by making the corners warmest. The temperature gradients are smallest at the corners in both cases. Hence, it is expected that the highest distortions and residual stresses shift from the corners to the center as the  $h$  changes from uniformity to the realistic nonuniformities considered here.

## EXAMINATION OF NUMERICAL FLOW MODEL SUITABILITY

To obtain the high heat transfer coefficients needed for quenching, high gas velocities and pressures are needed, resulting in flow Reynolds numbers of  $10^5 - 10^7$ . The flow is thus highly turbulent, and furthermore goes through separation and formation of complex wake-type regions. In typical quenching furnaces the approaching flow is anisotropic and contains some degree of turbulence already. Modeling and understanding are significantly complicated further by the fact that in many cases the quenched objects are stacked in some manner in a basket or on a grid, with wakes from one forming the upstream flow of the other.

In an effort to identify a reasonable way for predicting the distribution of  $h$  along the body surface, we have focused on several variants of the  $k$ - $\epsilon$  model (cf. Launder and Spalding, 1974), which is currently probably still the only practical model for solving turbulent flow problems in realistic applications. At the same time, while these models often account reasonably well for some of the overall flow parameters such as the pressure coefficient, we and others have found that they typically produce large errors in the prediction of the  $h$  distribution.

$k$ - $\epsilon$  turbulence modeling is only applicable in high  $Re$  regions, and it must be modified in regions close to the wall where the local Reynolds number is low. Further difficulties are known to occur in separated and recirculating flow regions (cf. Patel et al., 1985, Heyerichs and Pollard, 1996).

A popular method to render the  $k$ - $\epsilon$  model useful near the wall is Low Reynolds Number Modeling, exemplified by the Launder and Sharma (1974) model (LS). Yap (1987) has proposed a modification to the LS model (LSY) to improve the prediction in flows with adverse pressure gradients. It is known that this model

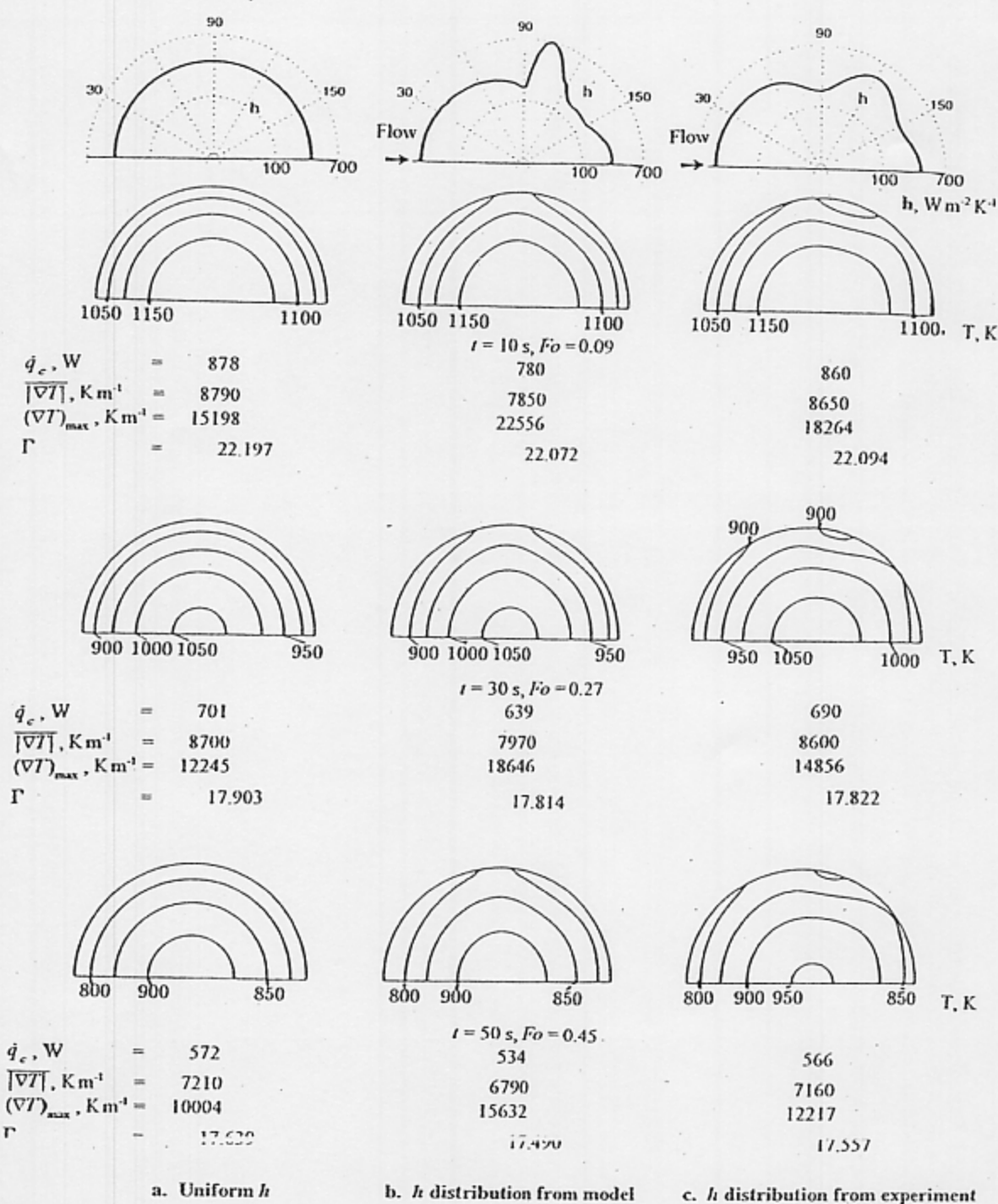


Figure 2: Comparison of the transient temperature distributions inside a stainless steel cylinder at  $T_{Li} = 1200 \text{ K}$ , for  $h$  distributions: (a) assumed uniform, (b) computed by us, for nitrogen at 10 bar, 300 K, and (c) experimentally-obtained (Žukauskas and Žiugžda, 1984). Figures 2b and 2c are during cross-flow quenching by gas at  $Re = (3.16)10^5$ ,  $Pr = 0.7$ ,  $k_f = 20 \text{ W m}^{-1} \text{ K}^{-1}$ ,  $Bi = 0.66$ .



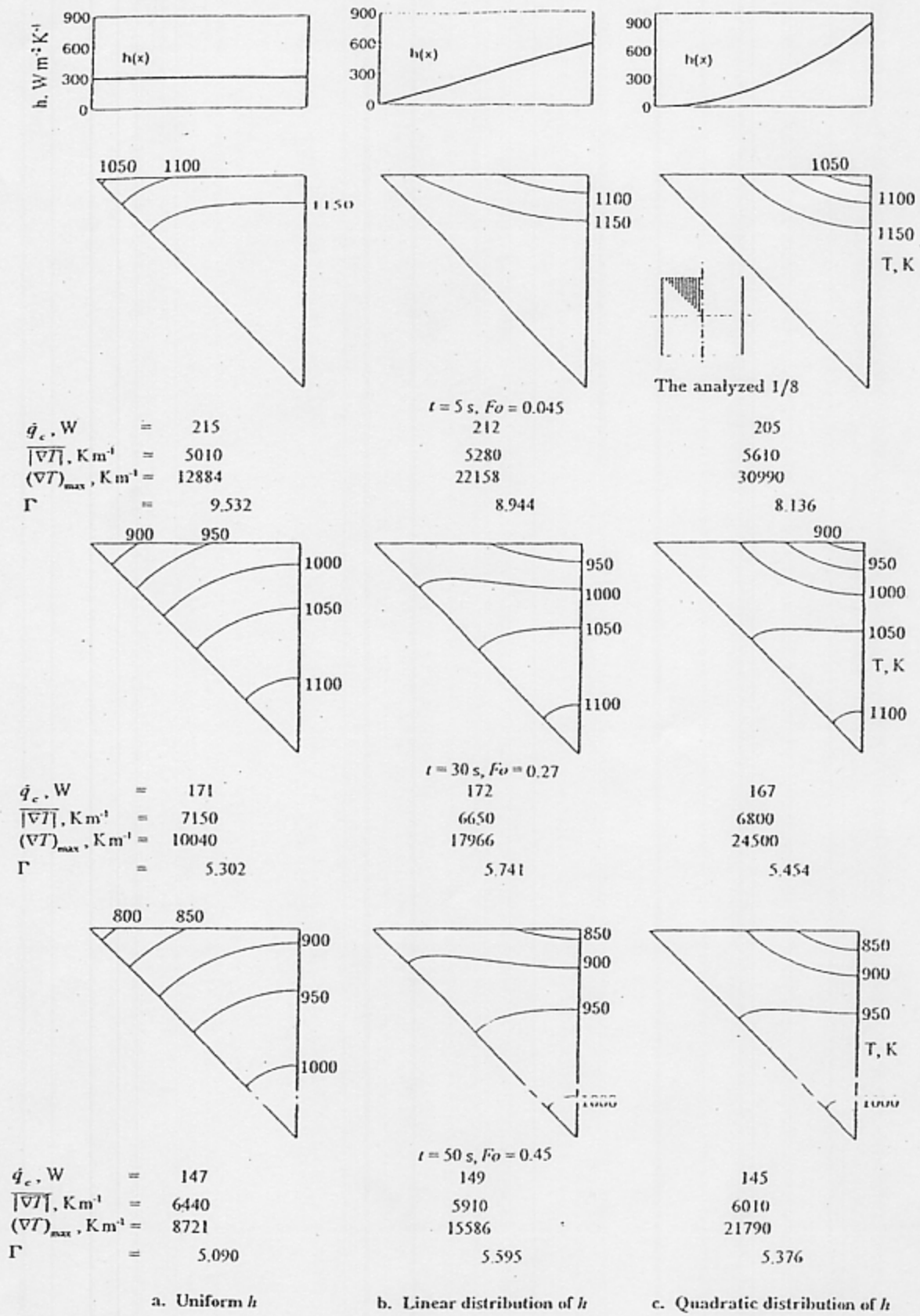


Figure 3: Comparison of the transient temperature distributions inside a stainless steel square rod at  $T_{\infty} = 1200 \text{ K}$ ,  $k_s = 20 \text{ W m}^{-1} \text{K}^{-1}$  (steel),  $Bi = 0.45$ , for given  $h$  distributions: (a) uniform, (b) linear, and (c) quadratic. As sketched in the inset, 1/8 of the rod cross section is shown, with the vertical line being its centerline.

predicts well flows in which the transition is close to the forward stagnation point. Further modifications, proposed by Cho and Goldstein (1993) (LSY-CG) with particular concern for recirculating flows, include employment of the Yap correction term but only when it is positive, thus avoiding the physically-unreasonable possibility that dissipation may be negative. A brief summary of these corrections, all having been confined to the additional term  $\bar{E}$  in the LS dissipation ( $\epsilon$ ) equation (cf. Heyerich and Pollard, 1996, eq. 7), is given in Table 1.

TABLE 1

The differences between the three  $k-\epsilon$  models compared here.

The Model	$\bar{E}$
LS	$2 \frac{\mu \mu_t}{\rho} \left( \frac{\partial^2 u}{\partial y^2} \right)^2$
LSY	$2 \frac{\mu \mu_t}{\rho} \left( \frac{\partial^2 u}{\partial y^2} \right)^2 + 0.83 \rho \frac{\bar{\epsilon}^2}{k} (d - 1) d^2$
LSY-CG	As LSY but 2 <sup>nd</sup> term used only if $d \geq 0$

where  $d \equiv k^{1/2}/c_y \epsilon$ .

The numerical analysis was performed by using the commercial finite-difference code CFX (AEA Technology, 1994). The object chosen was a cylinder, for which experimental data is available for comparison. The  $Re$  for the computations was chosen to be one in which the flow is steady, with a low free-stream turbulence of 1.2%. A graduated grid, with at least 80 points in the boundary layer region, as recommended in the literature, was chosen. Convergence was checked by (1) iteration until the residuals were reduced 1000-fold, and then, (2) grid independence was checked by changing from the second-order scheme to a first-order one. If then the residuals did not change and continued to diminish, the grid used was considered to be satisfactory.

Figure 4 shows the comparison of the distributions of  $h$  as computed by these three turbulent flow models and as obtained experimentally by Žukauskas and Žiugžda (1984). The commonly-used LS model predicts  $h$  reasonably well from stagnation to about 90°, but overpredicts it significantly (up to about 500%) further downstream, especially in the separated wake region. The LSY model, on the other hand overpredicts  $h$  significantly upstream, up to approximately the separation point but gives results which are within about 10% from the experimental ones in the wake region. The LSY-CG model is overall the best of the three, with the same accuracy as the LS model up to 90° and with an underprediction of up to about 40% in the separated flow region.

Models of turbulent flow over solid bodies are often judged by their ability to predict some characteristic flow parameters. We have confirmed that the errors which the models produce in predicting the pressure coefficient are significantly different from those they produce in predicting  $h$ . Overall, the LSY-CG model was still to be the best among the three models compared even in

predicting the pressure coefficient.

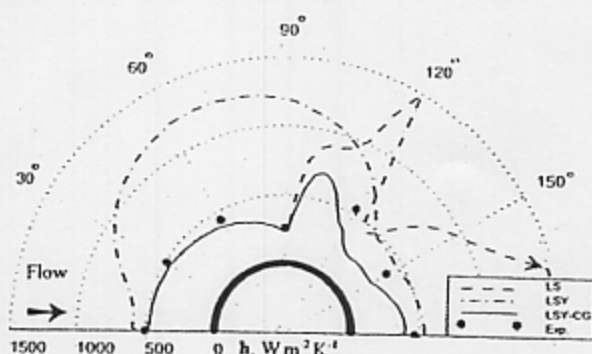


Figure 4: Comparison of the distributions of convective heat transfer coefficients in cross-flow gas-quenching of a cylinder at  $T_u=1200K$ , as computed by three versions of the  $k-\epsilon$  model and as determined experimentally by Žukauskas and Žiugžda (1984).  $Re = (3.16)10^5$ ,  $Pr = 0.7$ . The computations were for nitrogen at 10 bar, 300 K.

## CONCLUSIONS AND RECOMMENDATIONS

- The magnitude of the maximal temperature gradient in the quenched body is highly sensitive to the local magnitude of the convective heat transfer coefficient  $h$ .
- The maximal temperature gradients occur on the body surface, where  $h$  is maximal.
- The temperature distributions and gradients in the quenched body can be controlled by flow manipulation
- Two of the most popular  $k-\epsilon$  models we have examined, LS and LSY, have produced unacceptably large errors in the distributions of  $h$  around a cylinder in highly turbulent flow; the third one we have adapted, LSY-CG, predicts it much better overall but still has local errors of up to -40% which occur in the separated region. This error remains significant since, as shown with the cylinder, even a relatively small increase in nonuniformity due to numerical model inadequacy is seen to cause an increase of up to 28% in  $(\nabla T)_{max}$ .
- It is encouraging that there we have been able to adapt a  $k-\epsilon$  model (LSY-CG) which predicts  $h$  distributions with errors acceptable for at least rough estimation of the interior temperature profiles, but further search for and development of turbulent flow and heat transfer models which reduce the prediction error is recommended.
- It was not possible to foresee the  $h$ -prediction accuracy of these  $k-\epsilon$  models by the knowledge of their accuracy in predicting flow parameters such as the pressure coefficient: the errors which they produce in predicting these heat transfer and flow parameters are significantly different.

## NOMENCLATURE

- $A_s$  surface area of the quenched part,  $m^2$
- $Bi$  Biot number,  $= hL_c/k_s$
- $c_f$  length scale constant in  $\bar{E}$
- $\bar{E}$  the additional term in the turbulence dissipation equation
- $Fo$  Fourier number,  $= \alpha t/L_c^2$
- $h$  the local surface convective heat transfer coefficient,  $= \dot{q}_{c,s}/\Delta T_{s,f}$ ,  $W m^{-2} K^{-1}$

$k$	turbulent kinetic energy, $\text{m}^2 \text{s}^{-1}$
$k_s$	thermal conductivity of the solid, $\text{W m}^{-1} \text{K}^{-1}$
$L$	side of the square rod, m
$L_c$	characteristic dimension of the body: $R$ for the cylinder, $L/2$ for the square rod
$Pr$	Prandtl number for the gas, $\nu/\alpha$
$\dot{q}_s$	the overall convective heat loss from the surface, W
$\dot{q}_{s,i}$	local convective heat flux at the solid surface, $\text{W m}^{-2}$
$r$	radial coordinate, m
$R$	radius of the cylinder, m
$Re$	Reynolds number, $u_i L_c / \nu$
$t$	time, s
$T$	temperature, K
$T_g$	temperature of the cooling gas, K
$T_{s,i}$	initial temperature of the solid, K
$T_{s,t}$	The local temperature at the solid surface, K
$y$	coordinate normal to the solid surface, m
$u$	the velocity component in the free stream direction
$v$	the velocity component in direction perpendicular to $u$
$u_i$	the upstream inlet velocity, $\text{m s}^{-1}$
$U^*$	dimensionless velocity, $(u^2 + v^2)^{0.5} / u_i$
$V$	volume of the quenched part, $\text{m}^3$
$\Delta T_{s,t}$	the local temperature difference between the solid surface and the far fluid, $\equiv T_{s,t} - T_g$
$\epsilon$	the dissipation variable used in the $k-\epsilon$ model, $\text{m}^2 \text{s}^{-3}$
$\Gamma$	a heat treatment merit number, $\equiv \frac{\dot{q}_s (A_s/V)^2}{k  \nabla T }$
$\mu$	the molecular dynamic viscosity, $\text{kg m}^{-1} \text{s}^{-1}$
$\mu_t$	the turbulent dynamic viscosity, $\text{kg m}^{-1} \text{s}^{-1}$
$\nu$	kinematic viscosity of the gas, $\text{m}^2 \text{s}^{-1}$
$\phi$	azimuthal angle, °
$(\nabla T)_{\max}$	maximal temperature gradient in the solid body, $\text{K m}^{-1}$
$ \nabla T $	the volumetric average of the absolute temperature gradients in the solid, $\equiv \frac{1}{V} \int_V  \nabla T  dV$ , $\text{K m}^{-1}$

## REFERENCES

- AEA Technology, CFX version 4.1, Harwell Laboratory, Oxfordshire, OX 11 0RA, UK
- Bodin, J. and Segerberg, S., 1992, Variation in Heat Transfer Coefficient around Components of Different Shapes during Quenching, *Proc. Quenching & Distortion Control Conf.*, ASM Int., pp.165-170
- Cho, H.H. & Goldstein, R.J. 1993. An Improved Low-reynolds-number  $k-\epsilon$  Turbulence Model for Recirculating Flows, *Int. J. Heat Mass Transfer*, vol 37 pp.1795-1508.
- Dowling, W., Jr., Pattok, T., Ferguson, B.L., Schick, D., Gu, Y.H. & Howes, M., 1996. Development of a Carburizing and Quenching Simulation Tool: Program Overview. *Proc. 2<sup>nd</sup> Int. Conf. on Quenching and the Control of Distortion*, ASM Int., pp.349-355.
- Fletcher, A. J., 1989. *Thermal Stress and Strain Generation in Heat Treatment*, Elsevier, Amsterdam.
- Heyerichs, K., & Pollard, A. 1995. Heat transfer in separated and impinging turbulent flows, *Int. J. Heat Mass Transfer*, vol. 39, pp.2358-2400
- Inoue, T. and Wang, Z., 1985. Coupling between Stress, Temperature and Metallic Structures during Processes Involving Phase Transformations, *Mat. Sci. Technol.*, vol. 1, pp.845-850.
- Inoue, T., Inoue, H., Uehara, T., Ikuta, F., Arimoto, K., & Igari, T., 1996. Simulation and Experimental Verification of Induction Hardening Process for Some Kinds of Steel. *Proc. 2<sup>nd</sup> Int. Conf. on Quenching and the Control of Distortion*, ASM Int., pp.55-62.
- Lauder, B.E. & Spalding, D.B. 1974 The Numerical Computation of Turbulent Flows, *Computer Methods in Applied Mechanics and Engineering* vol 3, pp.269-289.
- Lauder, B. E. & Sharma, B. I. 1974. Applications of the Energy Dissipation Model of Turbulence to the Calculation of Flow near a Spinning Disc. *Lett. Heat Mass Transfer*, vol. 1, pp.131-138.
- Lohrmann, M., Hoffmann, F. and Mayr, P., 1996. Abkühlintensität von Gasen in Wärme-behandlungsanlagen und deren Bestimmung, *HTM*, vol. 51, pp. 183-187.
- Midea, S.J., Holm, T., Segerberg, S., Bodin, J., Thors, T. and Swärstom, K., 1996. High Pressure Gas Quenching-Technical and Economical Considerations. *Proc. 2<sup>nd</sup> Int. Conf. on Quenching and the Control of Distortion*, ASM Int., pp.157-163.
- Sjöström, S., 1985. Interactions and Constitutive Models for Calculating Quench Stresses in Steel, *Mat. Sci. & Technol.*, vol. 1, pp.823-829.
- Thuvander, A. & Melander A. 1993, Prediction of Distortion and Residual Stresses of Engineering Steels due to Heat Treatment. *2nd ASM Heat Treatment and Engineering Conference*, Dortmund, Germany
- Yao, C. 1987. Turbulent and Momentum Transfer In Recirculating and Impinging Flows. Ph.D. thesis, The Faculty of Technology, Manchester, U.K.
- Žukauskas, A. & Žiugžda, J. 1984 *Heat Transfer of a Cylinder in Crossflow*, Hemisphere, Washington, DC.

## ACKNOWLEDGMENT

This project was conducted at the Faxén Laboratory of the Royal Institute of Technology, Stockholm, with the support of AGA AB, SKF, and Volvo.